UCRL-90483 Rev. I
PREPRINT

JXB HEATING BY VERY INTENSE LASER LIGHT

W. L. Kruer
Kent Estabrook

This paper is being prepared for submittal to the Physics of Fluids

August 27, 1984

Lawrence Livermore National Laboratory

JXB HEATING BY VERY INTENSE LASER LIGHT*

W. L. Kruer and Kent Estabrook
University of California
Lawrence Livermore National Laboratory
Livermore, CA 94550

Abstract

Plasma heating by the oscillating component of the ponderomotive force of a very intense light wave is discussed.

*Work performed under the auspices of the U. S. Department of Energy by the Lawrence Livermore National Laboratory under contract number W-7405-ENG-48.

The absorption of very intense light is a problem of great interest to anyone studying ICF applications of CO_2 lasers. There is, of course, the well-known mechanism of resonance absorption,[1] which can be strongly enhanced by both cratering[2] and rippling[3] of the critical density surface. We have recently explored another little-known mechanism, which can play a significant role at the very high intensities commonly used in CO_2 experiments. This so-called $\underline{J}\mathrm{X}\underline{B}$ heating[4] is due to the electrostatic field driven by the oscillating component of the ponderomotive force of the laser light. Here we present a model calculation to show that the driven electrostatic field is sizable for high-intensity light. We then present computer simulations of the $\underline{J}\mathrm{X}\underline{B}$ heating, which demonstrate significant absorption of very intense light into electrons with a modest temperature.

We begin with a model calculation to illustrate the physics of this coupling mechanism. Consider a linearly polarized light wave with electric field amplitude $\underline{E} = E_L(x)(\sin \omega_o t)y$. The ponderomotive force, $\underline{f}_p$, exerted by this field is readily derived in the usual way to be

$$\underline{f}_p = - \frac{m}{4} \frac{\partial}{\partial x} v_L^2 (x) (1 - \cos 2\omega_o t) x , \tag{1}$$

where $v_L = eE_L/m\omega_o$, and, for simplicity, we have neglected thermal and relativistic effects. The time-averaged part produces steepening of the density profile, and the oscillating component can lead to heating. In effect, the oscillating ponderomotive force corresponds to driving the plasma with an electrostatic field E_d, where

$$\frac{eE_d}{m} = \frac{1}{4} \frac{\partial}{\partial x} v_L^2 (x)(\cos 2\omega_o t) \quad . \tag{2}$$

Since the magnitude of E_d is proportional to $v_L \partial v_L/\partial x$, significant absorption is expected only for very intense light.

To estimate the size of the driver field, we consider an intense planar light wave normally incident on an inhomogeneous slab of plasma and use the model of Lee et al.[5] to compute $E_L(x)$ in the strongly steepened light-plasma interface. For intense fields, the density variation is large, and a numerical solution of the model equations is needed. Figure 1 shows a typical result for the spatial variation of the amplitude of the transverse electric field and the plasma density in the interface. For this example, $(v_{FS}/v_e)^2 = 10$, where $v_{FS} = eE_{FS}/m\omega_o$, E_{FS} denotes the free-space value of E_L, and v_e is the electron thermal velocity. As expected from the pressure balance, the plasma is steepened by the intense, reflecting light wave to a density of $n_c(v_{FS}/v_e)^2$, where n_c is the critical density. Both the transverse field and the density vary quite rapidly in the interface.

Given $v_L(x)$, we can evaluate the magnitude of the driver field due to the oscillating ponderomotive force. For example, at the location where the driver field would be most enhanced by the plasma response ($n \approx 4n_c$), we find that

$$\frac{eE_d}{m} \approx 0.6\left(\frac{v_{FS}}{v_e}\right)^{1.8} \frac{v_e^2\omega_o}{c} \quad . \tag{3}$$

Although relativistic effects should be included for more quantitative estimates, the magnitude of this field is clearly significant when the incident light is very intense. The oscillating electrostatic field has a strong spatial variation in the light-plasma interface and will heat electrons that interact nonadiabatically with it.

To compute the absorption and electron heating, we have carried out computer simulations using a 1.5-dimensional particle code with electromagnetic fields and relativistic particle dynamics. In our simulations, we consider the propagation of an intense, planar light wave from vacuum onto a plasma slab. The plasma begins as an overdense slab with density equal to the upper density expected in the final steepened state; i.e.,

$n/n_c = (v_{FS}/v_e)^2$. The reflected light waves are allowed to escape into vacuum at the left boundary, and heated electrons are replaced with incoming thermal electrons at the right boundary. The evolution is followed until a quasi-steady state is attained.

Our simulations demonstrate significant heating when the light is very intense. As illustrated by the plot of electron phase space in Fig. 2, electrons are accelerated and then beamed into the plasma by the oscillating ponderomotive force. The effective temperature of the heated electrons is relatively modest, as shown by the plot of the electron distribution function in Fig. 3. In this example, the product of incident intensity and wavelength squared is 10^{18} Wμm^2/cm^2 (i.e., $I \approx 10^{16}$ W/cm^2 for CO_2 light), and the initial electron temperature of the dense plasma slab is 4 keV. The time-averaged absorption is about 11%. Note that the heated temperature is about 50 keV.

Table I shows the averaged absorption measured in a number of simulations with different incident intensities and background electron temperatures. As expected, the absorption is strongly dependent on intensity, ranging from 1 or 2% at $I\lambda_\mu^2 = 10^{17}$ Wμm^2/cm^2 to between 10 and 15% at $I\lambda_\mu^2 = 10^{18}$ Wμm^2/cm^2. A weak dependence of the absorption on background electron temperature is also evident.

Of course, these one-dimensional simulations of normally incident light are intentionally ideal to isolate this physical process. Two dimensional simulations of obliquely incident, p-polarized light show that resonance absorption is then quite efficient. The fractional absorption in a steepened profile peaks at about 50% for angles of incidence of about 20^0 and can be even larger when the critical surface becomes cratered and rippled. The heated electron temperature θ_h due to resonance absorption is quite large at high intensity; for example, $\theta_h \sim 200$ keV for $I\lambda_0^2 = 10^{18}$ W-μm^2/cm^2 and a background temperature of 4 keV. Two dimensional simulations of normally incident light would include the oscillating two stream and ion acoustic decay instabilities. Simulations[6] have indicated that the absorption due to these instabilities is modest in a steepened density profile, i.e., roughly 10% or less. The electrons are heated primarily along the electric vector of the light, in contrast to heating by resonance absorption and by the oscillating ponderomotive force discussed here. For comparison, we note that the oscillating ponderomotive force produces a fractional absorption of order 10% only when the light intensity is extremely large. The heated electrons are beamed inward and have a relatively modest temperature, given such a high light intensity. Since this process depends on the oscillating component of the ponderomotive force, we do not expect it to be strongly modified if resonance absorption and parametric instabilities are simultaneously operative.

In summary, we have demonstrated a novel mechanism for the absorption of very intense laser light. The oscillating component of the ponderomotive force generates an electrostatic field, which leads to electron heating. A model calculation shows that the electrostatic field is sizable for very intense light. Computer simulations with a relativistic particle code demonstrate significant absorption into electrons with a relatively modest temperature.

References

1. D. W. Forslund, J. M. Kindel, K. Lee, E. Lindman, and R. L. Morse, Phys. Rev. A 11, 679 (1975), Kent Estabrook, E. J. Valeo and W. L. Kruer, Phys. Fluids 18, 1151 (1975).
2. A. B. Langdon, Bull. Am. Phys. Soc. 22, 1174 (1977); C. Randall and J. S. DeGroot, Phys. Rev. Lett. 42, 179 (1979), J. J. Thomson, W. L. Kruer, A. B. Langdon, C. E. Max and W. C. Mead, Phys. Fluids 19, 1733 (1976).
3. R. Sagdeev, Probl. Contr. Thermo. Reactions 2, 406 (1959); K. Estabrook, Phys. Fluids 19, 406 (1976); E. Lindman, Journal de Physique C6-9 (1977); W. W. Woo, J. S. DeGroot and C. Barnes, Phys. Fluids 23, 2291 (1980).
4. W. L. Kruer and K. Estabrook, Lawrence Livermore National Laboratory, UCRL-50021-76, (1977).
5. K. Lee, D. W. Forslund, J. M. Kindel and E. L. Lindman, Phys. Fluids 20, 51 (1977); for relativistic corrections, see M. Stroscio, K. Lee and E. Lindman, Phys. Fluids 21, 1509 (1978).
6. Kent Estabrook and W. L. Kruer, Phys. Fluids 26, 1888 (1983).

Figure Captions

Fig. 1 The spatial variation of the transverse electric field ($v_L = eE_L/m\omega_0$) and the plasma density in the light-plasma interface. For this example, $(v_{FS}/v_e)^2 = 10$.

Fig. 2 An electron phase space at $\omega_0 t = 80\pi$ from a computer simulation of $\underline{J} \times \underline{B}$ heating. The incident light intensity was $I\lambda_\mu^2 = 10^{18}\ \frac{W - \mu^2}{cm^2}$. The plasma was initially an overdense slab with density $n = 100 n_{cr}$, an electron temperature $\theta_e = 4$ keV, and an ion-electron mass ratio of 1836.

Fig. 3 A plot of the electron distribution at $\omega_0 t = 80\pi$ in a computer simulation of $\underline{J} \times \underline{B}$ heating. The parameters are those for Fig. 2.

Table I The time-averaged absorption measured in simulations with different incident intensities and background electron temperatures.

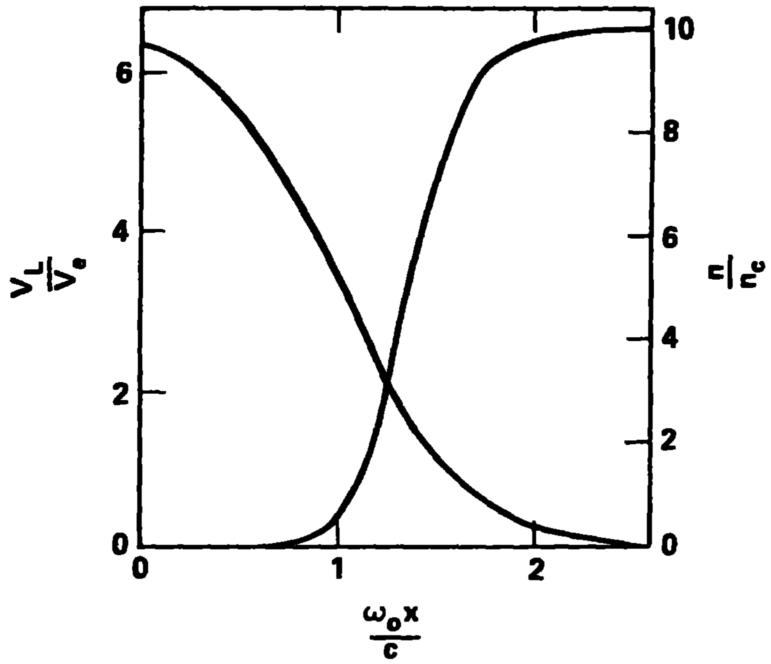

Fig. 1

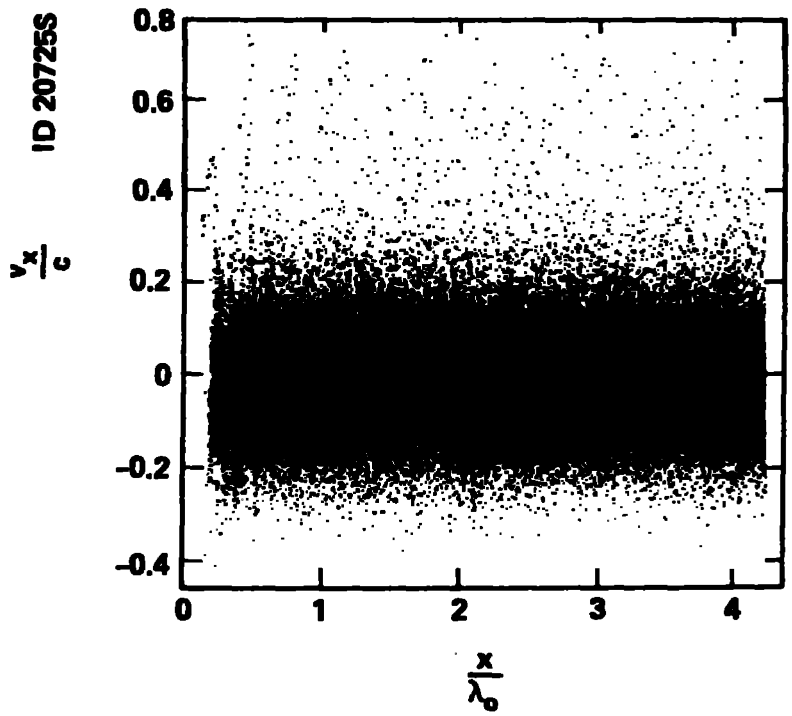

$I\lambda_0^2 = 10^{18}$, $T_e/T_i = 30$, $n/n_c = 100$

$T_e = 4$ keV, $m_i/m_e = 1836$, Time = 40 laser cycles

Fig. 2

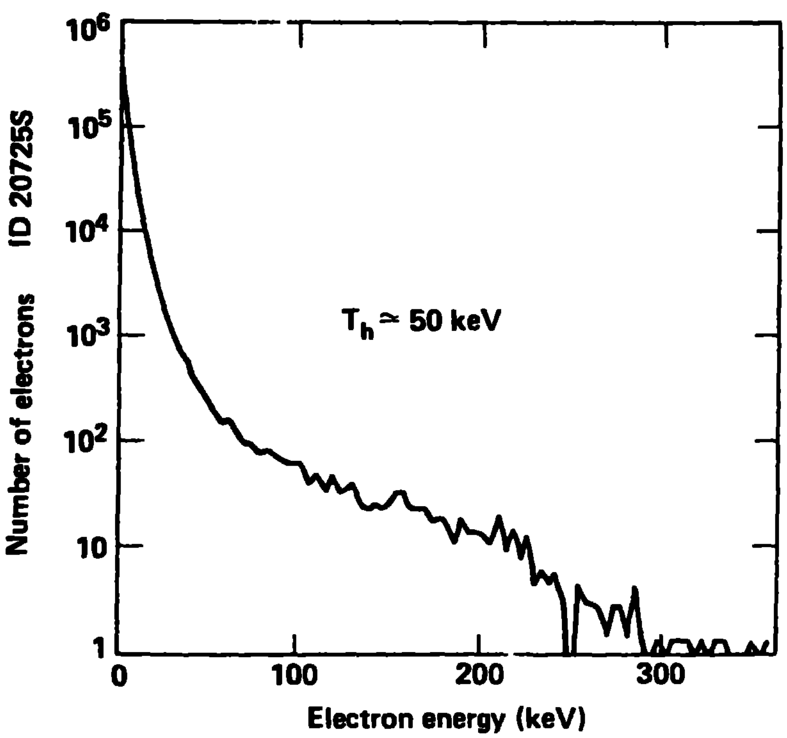

ID 207255
Number of electrons
Electron energy (keV)
$T_h \simeq 50$ keV
10^6
10^5
10^4
10^3
10^2
10
1
0
100
200
300

Fig. 3

T_e (keV)	$I\lambda_\mu^2$ ($W \cdot \mu m^2/cm^2$)	$f$abs
4	10^{17}	0.015
4	3×10^{17}	0.06
4	10^{18}	0.11
12	3×10^{17}	0.05
12	10^{18}	0.17
40	10^{18}	0.13

Table I